Atomic structure and stability of AlN(0001) and (000$\underline{1}$) surfaces

John E. Northrup and R. Di Felice
Xerox Palo Alto Research Center, 3333 Coyote Hill Road, Palo Alto, California 94304

Jörg Neugebauer
Fritz-Haber-Institut der Max-Planck-Gesellschaft, Faradayweg 4-6, D-14195 Berlin, Germany
(Received 16 December 1996)

We report first-principles calculations of the relative formation energies for possible reconstructions of the AlN(0001) and AlN(000$\underline{1}$) surfaces. Structural models with 2×2 symmetry and satisfying the electron counting rule, as well as metallic surfaces with 1×1 symmetry, have been considered. For AlN(0001) both Al-T4 and N-H3 adatom models are stable within the allowed range of the Al and N chemical potential: the N-adatom structure is stable in N-rich conditions and the Al-adatom structure is most stable in Al-rich conditions. For the AlN(000$\underline{1}$) surface the 2×2 Al-H3 adatom model is stable in N-rich conditions, while under Al-rich conditions a one-monolayer adlayer of Al is favored. [S0163-1829(97)04920-5]

Because of their applications as optoelectronic materials there is significant interest in understanding the electronic and structural properties of the group-III nitrides (AlGaInN). Epitaxial films are commonly prepared by growth on the basal plane of sapphire or Si-terminated SiC(0001) and this leads to a (0001) growth surface of the group-III nitride overlayer.[1–4] Recent first-principles density-functional calculations[5] have indicated that on the Si-terminated SiC(0001) surface AlN epitaxial films will grow with an (0001) polarity. Although knowledge of the local atomic structure is important for understanding and controlling the epitaxial growth process, there is very little information presently available on the (0001) basal plane surface structure of the III-V nitrides. One early study[6] has indicated a 2×2 reflection high-energy electron diffraction (RHEED) pattern following deposition of 30 nm of AlN on SiC(0001), but the local atomic structure has not yet been determined. A 2×2 RHEED pattern was also observed for AlN grown on a GaN buffer layer that was grown on SiC.[7] In a recent experimental study of GaN growth on sapphire,[8] using an ion-removed electron cyclotron resonance molecular-beam epitaxy technique, a 2×2 and a 4×4 reconstruction were observed during growth and during the cooling down, respectively. In this paper, we attempt to provide a comprehensive theoretical survey of possible structural elements that could give rise to the 2×2 reconstructions. The total energy and atomic structure for a variety of possible structures have been calculated within the local-density approximation (LDA) and the first-principles pseudopotential approach.

AlN adopts the wurtzite crystal structure with an in-plane hexagonal lattice constant $a=3.11$ Å and a c/a ratio of 1.60, a value which is slightly less than the ideal ratio, $c/a=(8/3)^{1/2}$. The electronegativities of Al and N are very different: 1.6 and 3.0, respectively, and so there is a significant ionic component to the bonding in AlN. The direct band gap is 6.2 eV. The atomic radii are 1.25 Å for Al and 0.70 Å for N. It is clear from a number of recent studies that atomic size mismatch plays an important role in governing the structural properties of point defects,[9] surfaces,[10] and extended defects[11] in GaN, and one expects similar behavior for AlN.

In light of previous structural studies for GaAs(111)2×2 (Refs. 12 and 13) and GaAs($\underline{111}$)2×2,[14,15] we have considered the adatom, vacancy, and trimer induced reconstructions that satisfy the electron counting rule. In addition to these structures, we also performed calculations for the ideally terminated 1×1 surface and a 1×1 surface with an additional monolayer of Al. Schematic representations of these structures are presented in Fig. 1.

We have performed calculations of the total energy and atomic structure within the local-density approximation and the first-principles pseudopotential approach. Forces and total energies were calculated in a plane-wave-based iterative procedure described by Stumpf and Scheffler.[16] The initial approximations to the wave functions were generated in a local-orbital scheme.[17] The surface is modeled in the repeated supercell approach. Each cell contains eight layers of AlN and the surface of one side of the layers is terminated with fractionally charged H atoms to saturate the bonds and prevent an unphysical charge transfer between the two ends of the slab. To saturate the Al dangling bonds on the (0001) surface, we employ H atoms of charge $\frac{5}{4}$ placed in atop sites above the Al atoms. To saturate the N dangling bonds on the (000$\underline{1}$) surface, we employ H atoms of charge $\frac{3}{4}$ placed in atop sites above the N. On the other side of the slab, the atomic positions in the top four layers, in addition to the adatoms (or adlayers), are allowed to relax. The plane-wave cutoff was taken to be 50 Ry and two special **k** points were employed in the Brillouin-zone sampling. The pseudopotentials for Al and N were generated in the Troullier and Martins[18] approach. With this pseudopotential for N and with the $1/r$ potential for H, we calculated the structural parameters for ammonia (NH_3) and found r(N-H)$=1.015$ Å and θ(H-N-H)$=107.0°$, in excellent agreement with the experimental values,[19] 1.012 Å and 106.7°. For the N_2 molecule we obtain a bond length of 1.075 Å, slightly less than the experimental value[19] of 1.098 Å. A theoretically determined in-plane hexagonal lattice constant of 3.04 Å was employed in the slab calculations for the AlN surfaces. This value is 2% smaller than the experimental lattice constant.

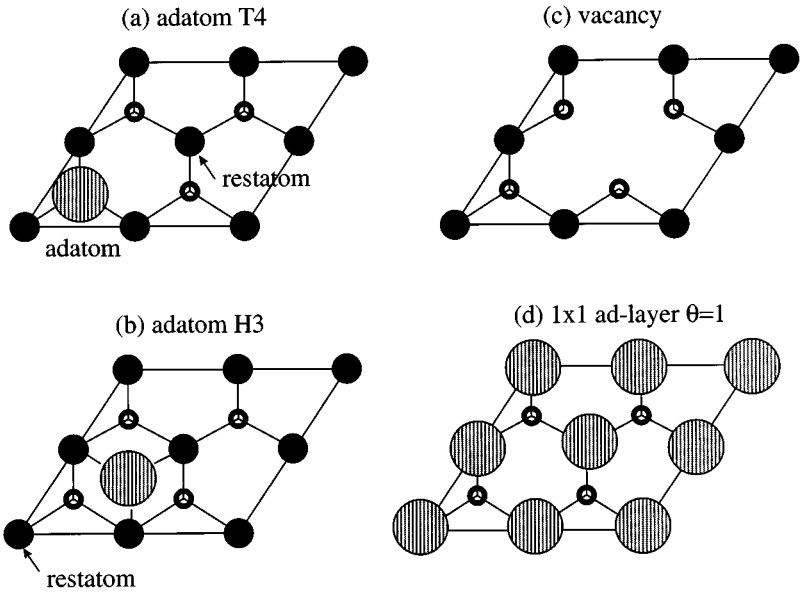

FIG. 1. Schematic representation of the 2 $\times$2 unit mesh (top view) showing the top two layers and the various structural elements. Filled circles denote Al atoms in the surface layer. Open circles denote N atoms in the second layer. Large shaded circles indicate Al adatoms and adlayer atoms. (a) Al-T4 adatom, (b) Al-H3 adatom, (c) Al vacancy, (d) 1$\times$1 Al adlayer.

We calculate the surface energy for the binary compound as a function of the chemical potential of one of its constituents (Al) within the thermodynamically allowed range at $T=0$.[20,21] The maximum chemical potential for Al is equal to the energy per atom of fcc Al, and we write this condition as $\mu_{\mathrm{Al}}<E(\mathrm{Al_{fcc}})$. In addition we know that the chemical potential of N must remain below the energy per atom of molecular nitrogen, the most stable elemental phase of nitrogen. We therefore have $\mu_{\mathrm{N}}<E(\mathrm{N_2})$. The chemical potentials of Al and N do not vary independently; their sum is equal to the energy per atomic pair in bulk AlN. We therefore have the condition $\mu_{\mathrm{Al}}+\mu_{\mathrm{N}}=2E(\mathrm{AlN_{bulk}})$. These conditions together imply that the minimum chemical potential of Al is $E(\mathrm{Al_{fcc}})-\Delta H$, where $\Delta H=E(\mathrm{Al_{fcc}})+E(\mathrm{N_2})-2E(\mathrm{AlN_{bulk}})$ is the heat of formation of AlN. From calculations of the total energy for fcc Al, the N_2 molecule and wurtzite AlN, we obtain $\Delta H=3.33$ eV, in excellent agreement with experiment: 3.3 eV.[22]

We begin by discussing the results for the nominally Al-terminated (0001) surface. Results for the surface formation energies, relative to that of the 2$\times$2 Al-vacancy structure, are plotted in Fig. 2. For the N adatom structure we have considered both the T4 and H3 adsorption sites[23] in the 2 $\times$2 unit cell and find that the N adatom prefers the H3 site over the T4 site by 3.3 eV/2$\times$2. The large difference in stability may be attributed to an electrostatic repulsion between the negatively charged N adatom and the second layer N atom that lies directly below the adatom in the T4 geometry (see Fig. 1). This repulsion is not present when the N adatom occupies the H3 site. The N adatom structure has the same stoichiometry as the Al vacancy structure (one may be converted to the other by exchanging one AlN pair with the bulk). As indicated in Fig. 2 the N-H3 adatom is lower than the Al vacancy by 0.61 eV/2$\times$2 cell. Under N-rich conditions the N-adatom model is the most stable structure of those we have examined.

Under Al-rich conditions we find that the Al adatom, in the T4 site, is the most energetically favorable 2$\times$2 structure. For the Al adatom, the T4 site is preferred over the H3 site by about 0.8 eV/adatom. Other structures do not appear to be stable for any values of the Al chemical potential. For example, the N-trimer structures are quite unstable. Structures containing $\frac{3}{4}$ monolayer of Al, forming weakly bonded trimers, or a full adlayer of Al remain higher in energy than the Al-adatom structure up to the maximum possible Al chemical potential. However, under very Al-rich conditions we see in Fig. 2 that the 1$\times$1 structure comprised of an adlayer of Al atoms becomes competitive in energy with the

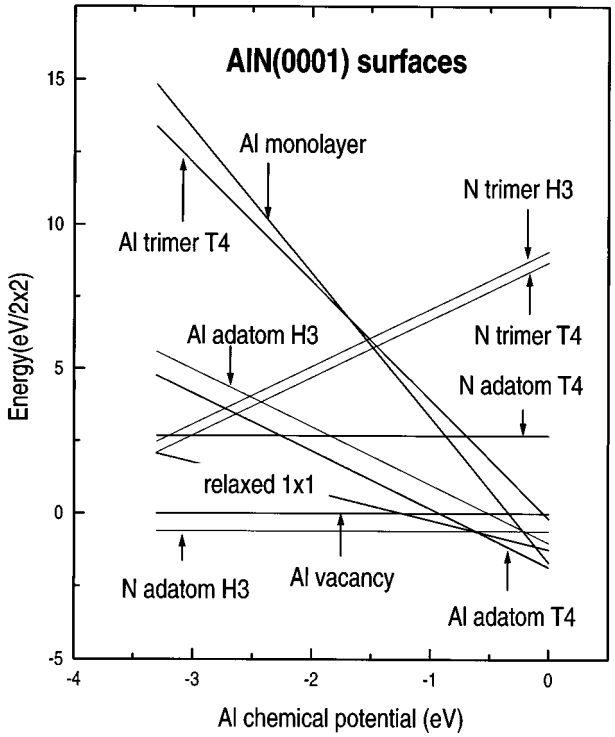

FIG. 2. Relative formation energies for the AlN(0001)2$\times$2 surfaces. The chemical potential of Al varies between $\mu_{\mathrm{Al(bulk)}}-\Delta H<\mu_{\mathrm{Al}}<\mu_{\mathrm{Al(bulk)}}$. $\Delta H=3.3$ eV and $\mu_{\mathrm{Al(bulk)}}\equiv 0$.

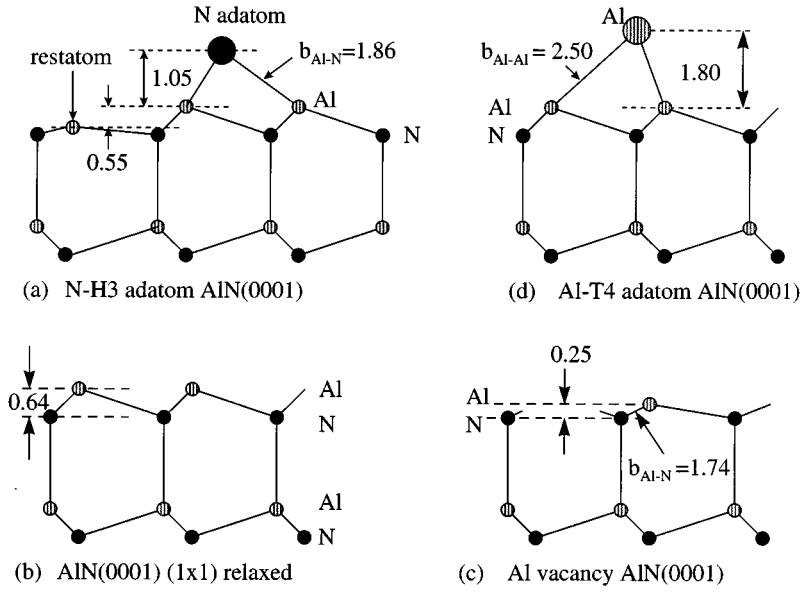

FIG. 3. Schematic structural models for the AlN(0001) surfaces. Distances are expressed in Å. (a) N-H3 adatom model. (b) Ideal topology 1×1 surface. (c) Al-vacancy model. (d) Al-T4 adatom model.

Al adatom. This result suggests that under Al-rich growth conditions it may be possible to achieve Al coverages approaching one monolayer.

Because there are two possible stable 2×2 reconstructions within the allowed range of Al chemical potential, it is not possible for theory alone to decide whether the observed 2×2 reconstructions correspond to the N adatom or to the Al adatom. Further experimental work, such as scanning tunneling microscopy or low-energy electron diffraction, is required. Angle-resolved photoemission and inverse-photoemission experiments would also provide important information. To provide motivation and guidance for these experiments we have calculated the surface-state electronic structure for several structures. Because these band structures are based on eigenvalues of the Kohn-Sham equations rather than on quasiparticle calculations,[24] the energy gaps and alignment of the bands with respect to the valence-band maximum are somewhat uncertain. For example, the calculated bulk band gap for AlN is 4.9 eV, approximately 1.3 eV less than the experimental value. The lower value can be attributed to the use of the LDA eigenvalues.[25] Nevertheless, we expect the overall characteristics of the calculated surface state spectrum to be sufficiently reliable to allow a structural determination based on a comparison of these results with spectroscopic data. Below we briefly discuss the atomic and electronic structure for the N adatom, the 1×1 ideal surface, the Al vacancy, and the Al adatom structure. For each of these structures the calculations show the existence of both occupied and empty surface states deep inside the fundamental energy gap.

The atomic structure obtained for the *N adatom H*3 structure is indicated schematically in Fig. 3(a). The adatom is located 1.05 Å above the plane of its three Al neighbors with a corresponding Al-N bond length of 1.86 Å. A significant amount of distortion is present within the top layer of Al, and the Al restatom is located 0.55 Å below the plane of the three other atoms in the topmost Al layer. The $3p_z$ orbital on the Al restatom gives rise to an unoccupied band of surface states in the upper part of the band gap. The $2p$ orbitals of the N adatom give rise to three occupied bands in the lower part of the gap as shown in Fig. 4(a).

For the *relaxed 1×1 ideal-topology structure* the Al atoms in the surface layer deviate only slightly from their ideal positions. The interlayer spacing of the outermost N-Al bilayer increases by $\sim$0.02 Å. A schematic model of the structure is shown in Fig. 3(b). The Al $3p$ states give rise to a partially filled band of surface states located deep inside the bulk band gap of AlN, as shown in Fig. 4(b). In this hypothetical structure, the surface would be metallic with a Fermi energy located about 3.5 eV above the valence-band maximum (VBM).

The *Al-vacancy structure* is formed by removing one Al atom from each 2×2 unit cell. Electrons are then transferred from the Al to the N dangling bonds, and the Al atoms attempt to achieve an sp^2 bonding configuration. This corresponds to a vertical relaxation of the surface Al atoms and the N-Al bilayer spacing is compressed from the ideal value, 0.62 Å, to about 0.25 Å as indicated in Fig. 3(c). This vertical relaxation leads to a contraction of the bonds between the threefold-coordinated Al and N atoms from the bulk value 1.86 Å to 1.74 Å. This 6% contraction of the bond is quite similar to that found for the AlN($10\underline{1}0$) (Ref. 26) and GaN($10\underline{1}0$) surfaces.[12] The relaxation leads to a reduction in electrostatic energy without a rehybridization of the threefold-coordinated N atoms. In the Al-vacancy structure there are three empty Al dangling bonds and three occupied N dangling bonds in each unit cell. The calculated surface states are shown in Fig. 4(c). Three bands of occupied surface states, derived from the threefold-coordinated N atoms, are located in the energy range between 0 and 2 eV above the VBM. The rather large energy width of the occupied vacancy state manifold is a consequence of the coupling of the N-$2p$ orbitals in the (0001) plane. Three empty bands of surface states derived from the Al-$3p$ orbitals are found in the upper part of the energy gap.

For Al-rich conditions we find that the 2×2 *Al-T4 adatom structure* is the most stable structure. The length of the Al-Al bonds between the adatoms and the surface-layer at-

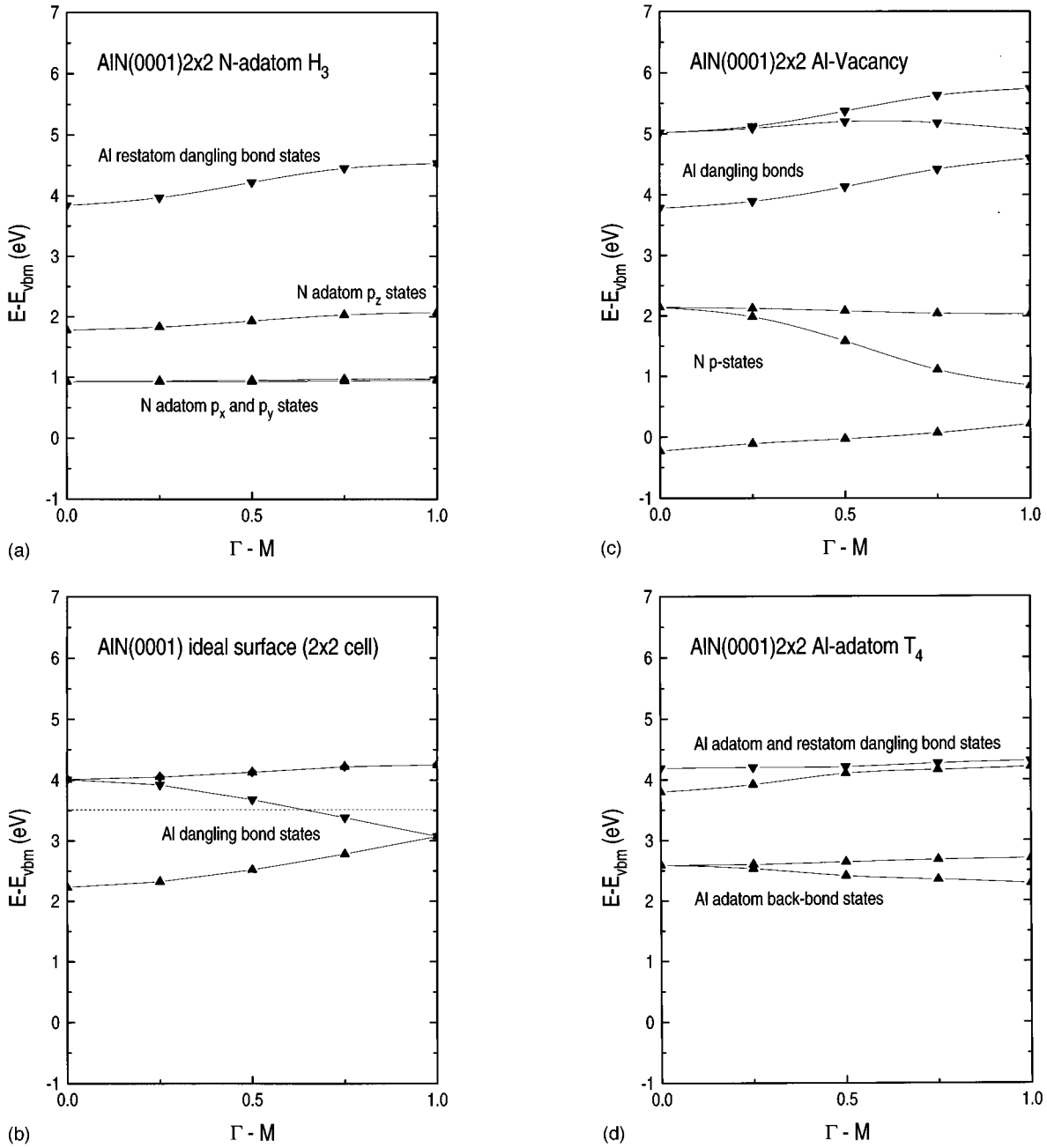

FIG. 4. Surface-state energies for AlN(0001) surfaces are plotted from Γ to M. M is the midpoint of the edge of the 2×2 Brillouin zone. Energies are given relative to the bulk valence-band maximum of AlN. The bulk band-gap energy is 4.9 eV. (a) Surface states for the N-H3 adatom model. The three surface bands derived from the N-$2p$ orbitals are fully occupied while the band derived from the Al-$3p_z$ orbital on the restatom is empty. (b) Surface states for the 1×1 ideal-topology surface. The bands are folded into a 2×2 Brillouin zone. The uppermost branch is doubly degenerate and the Fermi energy is located at 3.5 eV above the valence-band maximum. (c) Surface states for the Al vacancy model. Three Al-derived dangling bond states are empty and three N-derived states are fully occupied, but lie above the valence-band maximum. (d) Surface states for the Al-T4 adatom model. The two Al-Al back-bond states are occupied and the two Al dangling bond bands are empty.

oms is 2.50 Å. This distance is close to twice the atomic radius of Al. The adatom is located 1.80 Å above the plane of its three Al neighbors as indicated in Fig. 3(d). For this structure the distorted back bonds of the adatom give rise to two bands of occupied states located about 2.5 eV above the VBM as shown in Fig. 4(d). The Al adatom and restatom dangling bonds give rise to two unoccupied bands located approximately 4 eV above the VBM.

We turn now to a discussion of the results obtained for the $(000\underline{1})$ surface that is nominally terminated by an outermost N layer. The relative surface formation energies for the various structures examined are shown in Fig. 5. The N-adatom and N-trimer structures are very high in energy and can be eliminated as possible structures. The relaxed 1×1 structure, having a full monolayer of threefold-coordinated N atoms in the last bilayer is also very high in energy. We find that the N-vacancy and the Al-T4 adatom structures have nearly equal formation energies; the calculated difference is only

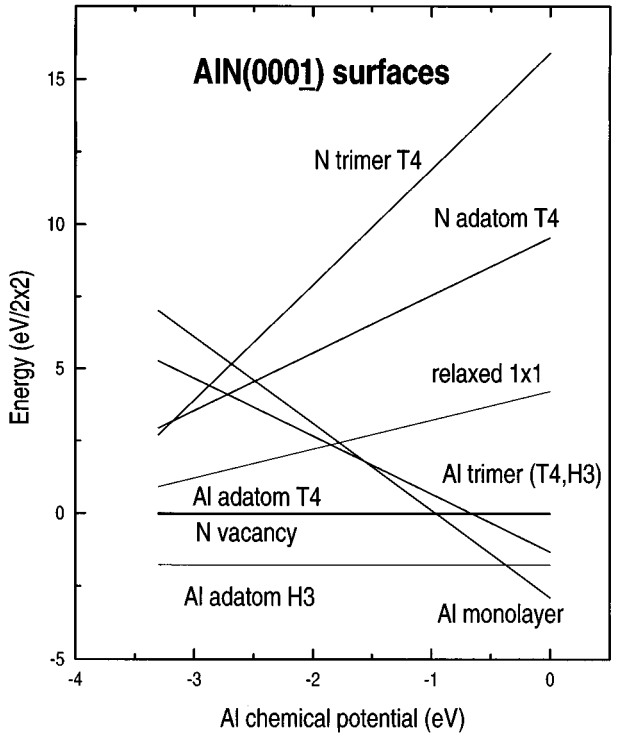

FIG. 5. Relative formation energies for the AlN(000$\underline{1}$)2×2 surfaces. The chemical potential of Al varies between $\mu_{\mathrm{Al(bulk)}}-\Delta H<\mu_{\mathrm{Al}}<\mu_{\mathrm{Al(bulk)}}$. $\Delta H=3.3$ eV and $\mu_{\mathrm{Al(bulk)}}\equiv 0$. The energies of the N vacancy and the Al-T4 adatom models are equal to within 0.1 eV/(2×2 cell). The energy of the Al-trimer structure is nearly independent of whether the trimer occupies the T4 or H3 position. The N adatom and trimer structures are relatively high in energy. Under N-rich conditions the Al-H3 adatom model is preferred. Under Al-rich conditions the 1×1 Al adlayer is lowest in energy among the structures tested.

$\sim$0.08 eV/2×2 with the N vacancy being slightly lower. On the (000$\underline{1}$) surface the Al adatom prefers the H3 binding site over the T4 site by about 1.8 eV/cell. The preference for the H3 adatom with respect to the T4 adatom binding site on the AlN(000$\underline{1}$)2×2 surface can be attributed to an electrostatic repulsion between the positively charged Al adatom and the positively charged second-layer Al atom. Over most of the allowed range of chemical potential we find the Al-H3 adatom model to be the most stable structure of those we have examined. Schematic models of the N vacancy and Al-H3 adatom models are shown in Figs. 6(a) and 6(b). In the N-vacancy structure the Al-N bonds between the threefold-coordinated N and Al atoms contract to 1.74 Å. This, again, represents a 6% contraction with respect to the bulk bond length. The bond contraction occurs as the threefold Al atoms relax towards an sp^2 bonding configuration.

For very high Al chemical potentials a 1×1 Al-adlayer structure is energetically favorable. In the adlayer structure, indicated schematically in Fig. 7, there is a full monolayer of Al in the atop site with an Al-N bond length of 1.88 Å, which is close to the bulk bond length. Because the 1×1 adlayer structure gives rise to a metallic electronic structure, and because the interatomic forces within the adlayer are expected to be weak, it seems likely that a Peierls instability will develop. Such an instability would lead to a reduction in

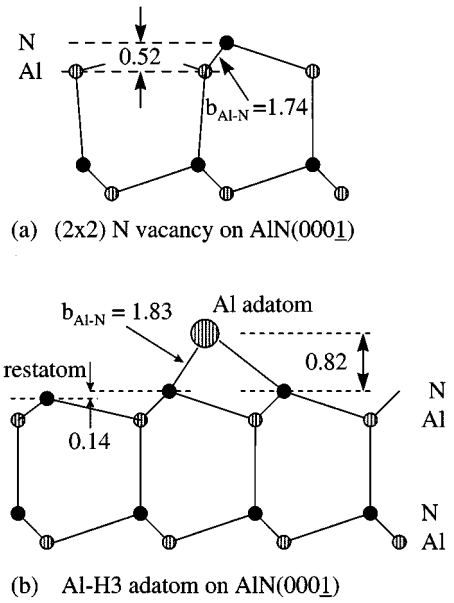

FIG. 6. (a) AlN(000$\underline{1}$)2×2 vacancy model. (b) AlN(000$\underline{1}$)2×2 Al-H3 adatom model. Distances are expressed in Å.

symmetry (denoted $n\times m$) and to the opening of an energy gap at the Fermi level. Since each Al in the adlayer contributes $\frac{3}{4}$ electron to the N atoms, to achieve a semiconducting band structure the $n\times m$ reconstruction must satisfy the condition $nm=(8,16,24,\ldots)$.

The calculations indicate that N-adatom and N-trimer structures are not stable under any conditions for the AlN(000$\underline{1}$) surface. This highlights the difference between the surfaces of the nitrides and the arsenides. On the GaAs($\underline{1}\underline{1}\underline{1}$) surface, As trimers give rise to a stable 2×2 reconstruction under As-rich conditions.[14,15] The calculated As-As bond length in the trimers is 2.44 Å,[15] which is nearly the same as the As-As distance in crystalline As ($\sim$2.5 Å). Thus the intratrimer bonding is quite strong in this case. However, within the N trimer the equilibrium N-N distance is 1.61 Å, which is about 50% larger than the equilibrium distance in the most stable form of elemental N, the N_2 molecule. Thus the relatively small size of the N atom precludes the stability of trimers on AlN(000$\underline{1}$) surfaces.

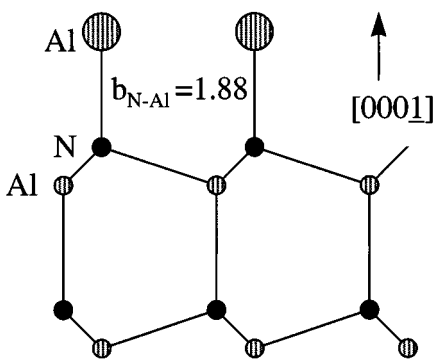

FIG. 7. AlN(000$\underline{1}$)1×1 Al-adlayer structure.

A common relaxation mechanism appears to be operative for the (0001) Al vacancy, the (000$\underline{1}$) N vacancy, and the (10$\underline{1}$0) surfaces of AlN (Ref. 26) and GaN.[12] Each of these reconstructions exhibit equal numbers of threefold-coordinated nearest-neighbor cations and anions, and in each case the threefold-coordinated cation relaxes by moving towards the sp^2 configuration and the anion-cation bonds contract by $\sim 6\%$. The N atoms, however, do not undergo a significant rehybridization. Calculations for the AlN(10$\underline{1}$0) surface,[26] for which there is one threefold Al and one threefold-coordinated N atom in each 1×1 unit cell, predict an absolute surface energy of $\sigma_{10\underline{1}0}=2.37$ eV/(1×1), which is equivalent to 157 meV/Å^2. From this result a rough estimate of the absolute surface energy of the AlN(0001) and the AlN(000$\underline{1}$) vacancy structures may be obtained. In each 2×2 unit cell of these vacancy reconstructions there exist three threefold-coordinated Al and N atoms having local atomic structures similar to their counterparts on the (10$\underline{1}$0) surface. Thus, a reasonable estimate of the surface energies of the (0001) and (000$\underline{1}$) vacancy surfaces is $3\sigma_{10\underline{1}0}=7.1$ eV/$(2\times2$ cell). From this, one may estimate the absolute energies of the structures shown in Figs. 2 and 5. For example, the AlN(000$\underline{1}$)2×2 Al-H3 adatom structure would have an estimated absolute energy of 5.3 eV/$(2\times2$ cell), corresponding to 165 meV/Å^2.

We may estimate the binding energies for adatoms on the (0001) and (000$\underline{1}$) surfaces by comparing the energies of the 2×2 adatom reconstructions with the energies of the ideal surfaces. In this approach we are neglecting the interactions between adatoms in the 2×2 array. In the Al-rich limit, corresponding to $\mu_{\mathrm{Al}}=\mu_{\mathrm{Al(bulk)}}$, we find the 2×2 Al-T4 adatom structure to be lower than the 1×1 ideal surfaces by 0.6 eV/adatom. Then, since the cohesive energy of bulk Al is 3.4 eV/atom we obtain an adatom binding energy of 4.0 eV on the (0001) surface. On the (000$\underline{1}$) surface the energy of the Al-H3 adatom surface is lower than the 1×1 N-terminated surface by 6.0 eV in Al-rich conditions. The Al-adatom binding energy is therefore estimated to be 9.4 eV on the (000$\underline{1}$) surface. Invoking similar approximations and employing the fact that the cohesive energy of molecular N_2 is 4.9 eV, we estimate that N adatoms are bound by 7.6 eV and 2.9 eV to the (0001) and (000$\underline{1}$) surfaces.

To summarize, for the AlN(0001)2×2 surface we find that the N-H3 adatom structure is energetically favorable for N-rich conditions, while an Al-T4 adatom structure appears to be the most probable for Al-rich conditions. On the AlN(000$\underline{1}$)2×2 surface the Al-H3 adatom structure is favored under N-rich conditions. Under Al-rich conditions a one monolayer Al adlayer is found to be the most stable structure.

This work was supported by the Office of Naval Research under Contract No. N00014-95-C-0169.

[1] J. L. Rouviere, M. Arlery, A. Bourret, R. Niebuhr, and K. H. Bachem, in *Gallium Nitride and Related Materials*, edited by R. D. Dupuis, J. A. Edmond, F. A. Ponce, and S. Nakamura, MRS Symposia Proceedings No. 395 (Materials Research Society, Pittsburgh, 1996).

[2] F. A. Ponce, D. P. Bour, W. T. Young, M. Saunders, and J. W. Steeds, Appl. Phys. Lett. **69**, 337 (1996).

[3] R. B. Capaz, H. Lim, and J. D. Joannopoulos, Phys. Rev. B **51**, 17 775 (1995).

[4] F. A. Ponce, C. G. Van de Walle, and J. E. Northrup, Phys. Rev. B **53**, 7473 (1996).

[5] R. Di Felice, J. E. Northrup, and J. Neugebauer, Phys. Rev. B **54**, R17 351 (1996).

[6] M. E. Lin, S. Strite, A. Agarwal, A. Salvador, G. L. Zhou, N. Terguchi, A. Rockett, and H. Morkoc, Appl. Phys. Lett. **62**, 702 (1993).

[7] M. A. L. Johnson *et al.*, J. Vac. Sci. Technol. B **14**, 2349 (1996).

[8] K. Iwata, H. Asahi, S. Yu, K. Asami, H. Fujita, M. Fushida, and S. Gonda, Jpn. J. Appl. Phys. **35**, L289 (1996).

[9] J. Neugebauer and C. G. Van de Walle, Phys. Rev. B **50**, 8067 (1994).

[10] J. E. Northrup and J. Neugebauer, Phys. Rev. B **53**, 10 477 (1996).

[11] J. E. Northrup, J. Neugebauer, and L. T. Romano, Phys. Rev. Lett. **77**, 103 (1996).

[12] S. Y. Tong, G. Xu, and W. N. Mei, Phys. Rev. Lett. **52**, 1693 (1984).

[13] D. J. Chadi, Phys. Rev. Lett. **52**, 1911 (1984).

[14] E. Kaxiras, Y. Bar-Yam, J. D. Joannopoulos, and K. C. Pandey, Phys. Rev. Lett. **57**, 106 (1986).

[15] D. K. Biegelsen, R. D. Bringans, J. E. Northrup, and L. E. Swartz, Phys. Rev. Lett. **65**, 452 (1990).

[16] R. Stumpf and M. Scheffler, Comput. Phys. Commun. **79**, 447 (1994).

[17] J. Neugebauer and C. G. Van de Walle, in *Materials, Theory, Simulations, and Parallel Algorithms*, edited by R. Kaxiras, J. Joannopoulos, P. Vashista, and R. K. Kalia, MRS Symposia Proceedings No. 408 (MRS, Pittsburgh, 1995).

[18] N. Troullier and J. L. Martins, Phys. Rev. B **43**, 1993 (1991).

[19] David R. Lide, *Handbook of Chemistry and Physics* (CRC Press, Boca Raton, 1995).

[20] Guo-Xin Qian, R. M. Martin, and D. J. Chadi, Phys. Rev. B **38**, 7649 (1988).

[21] J. E. Northrup, Phys. Rev. Lett. **62**, 2487 (1989).

[22] O. Kubaschewski and C. B. Alcock, *Metallurgical Thermochemistry* (Pergamon, Oxford, 1979).

[23] J. E. Northrup, Phys. Rev. Lett. **53**, 683 (1984).

[24] M. S. Hybertsen and S. G. Louie, Phys. Rev. Lett. **55**, 1418 (1985).

[25] A. Rubio, J. L. Corkill, M. L. Cohen, E. L. Shirley, and S. G. Louie, Phys. Rev. B **48**, 11 810 (1993).

[26] R. Di Felice *et al.* (unpublished).